**Rare Metal Materials and Engineering**
Volume 52, Issue 7, July 2023
Available online at www.rmme.ac.cn

Science Press

**Cite this article as**: Guo Tingbiao, Feng Rui, Li Kaizhe, et al. Hall-Petch Strengthening in Single Crystal Copper with High Conductivity During Cryo-ECAP[J]. Rare Metal Materials and Engineering, 2023, 52(07): 2396-2403.

ARTICLE

# Hall-Petch Strengthening in Single Crystal Copper with High Conductivity During Cryo-ECAP

**Guo Tingbiao[1,2], Feng Rui[1], Li Kaizhe[1], Gao Yang[1], Qian Danchen[1], Jia Zhi[1,2], Ding Yutian[1,2], Ling Dekui[3,4]**

*[1] State Key Laboratory of Advanced Processing and Recycling of Nonferrous Metals, Lanzhou University of Technology, Lanzhou 730050, China; [2] School of Materials Science and Engineering, Lanzhou University of Technology, Lanzhou 730050, China; [3] Jinchuan Group Co., Ltd, Jinchang 737100, China; [4] State Key Laboratory of Nickel and Cobalt Resource Comprehensive Utilization, Jinchang 737100, China*

**Abstract:** The deformation microstructure and texture evolution of single crystal copper after cryogenic equal channel angular pressing (Cryo-ECAP) process were characterized by optical microscope, scanning electron microscope, X-ray diffractometer, and electron backscatter diffraction. The mechanical properties and conductivity properties were analyzed. The microstructure transition mechanism and its effects on the mechanical properties and conductivity properties were discussed. Results show that the directional shear bands formed in the early stage of Cryo-ECAP process seriously affect the microstructure transformation during the subsequent deformation. With increasing the strain, a high-density dislocation pile-up is formed in the shear bands during deformation by route A, and the proportion of characteristic grain boundaries is increased. The dislocations in the shear bands during deformation by route $B_C$ present strong interactions, and the orientation of shear bands is dispersed after the deformation by route C. After 6 passes of deformation, the strong {111}<112> texture forms in the microstructure of single crystal copper, the strength increases from 126.0 MPa to 400.2 MPa, and the conductivity remains of above 98%IACS. After Cryo-ECAP, the directional shear bands form in the texture and the high-density dislocations are produced. The entanglement of dislocations effectively prevents the dislocation slip, and therefore the grains maintain the characteristics of single crystal.

**Key words:** single crystal copper; cryogenic equal channel angular pressing; microstructure; texture; mechanical properties; conductivity

Due to its excellent electrical conductivity, thermal conductivity, and ductility, single crystal copper attracts much attention in the electronics industry. However, the low strength severely restricts its application in the transportation, communication, and electronic information fields. Therefore, the methods to simultaneously maintain the high ductility and high conductivity and improve the strength of single crystal copper have been extensively researched[1–2]. The conventional strengthening methods cannot simultaneously improve the strength and conductivity of single crystal copper. Introduction of solid solution atoms into the matrix by alloying can effectively hinder the dislocation motion, thereby improving the material strength, but it may lead to the inhomogeneity of composition and deformation, which enhances the scattering of electrons and seriously reduces the conductivity of materials[3–5]. The increase in high angle grain boundaries caused by dislocation slip during plastic deformation is effective to improve the material strength, but to some extent causes a reduction in conductivity, which has the similar effect to that of alloying on conductivity[6]. The material strength can be significantly increased by grain refinement during general plastic deformation, but the dislocations are easily annihilated at grain boundaries due to the reduction in grain size, resulting in a significant reduction in ductility of material[7–8]. Jayakumara et al[9] found that the introduction of a large number of twins by pure shear deformation induced by twinning can simultaneously increase the strength and maintain the good thermal stability, high

Received date: September 25, 2022
Foundation item: National Natural Science Foundation of China (51861022, 51261016); 2020 Key Talent Projects of Gansu
Corresponding author: Guo Tingbiao, Ph. D., Professor, State Key Laboratory of Advanced Processing and Recycling of Nonferrous Metals, Lanzhou University of Technology, Lanzhou 730050, P. R. China, E-mail: lutguotb@163.com

Copyright © 2023, Northwest Institute for Nonferrous Metal Research. Published by Science Press. All rights reserved.

electrical conductivity, and fine thermal conductivity of materials. A large number of lamellar structures are formed in the single crystal microstructure during the equal channel angular pressing (ECAP) process, which induces the directional twinning and results in the twins with high density in the single crystal copper, thereby effectively improving the mechanical properties and maintaining the high conductivity of material[10]. Wu et al[11] investigated the deformation twinning behavior of single crystal copper during ECAP and found that the deformation twinning has strong orientation dependence. Higuera-Cobos et al[12] obtained the sub-micron grains through multi-pass extrusion of commercially pure copper by route $B_C$. A stable deformation microstructure is achieved after four passes, and the conductivity slightly decreases. Fukuda et al[13] found that the low angle subcrystalline cell structure parallel to the {111} <110> slip system is formed in the single crystal copper after one pass of ECAP.

However, the dislocation movement can be significantly hindered at cryogenic temperature. Thus, the stress required for thermal activation becomes larger, which is beneficial to improve the mechanical properties of materials[14–15]. Qin et al[16] successfully prepared ultrafine twins with thickness of about 10 nm by cryogenic rolling, which significantly improved the strength and hardness of Cu-Zn-Si alloy. Chen et al[17] found that the cryogenic ECAP (Cryo-ECAP) process can effectively inhibit the dynamic recovery in the grains of pure 1050 aluminum alloy. Cryogenic deformation promotes the twinning and dislocation accumulation, leading to the improvement of comprehensive properties. However, the single crystals are anisotropic, resulting in different patterns of orientation change after ECAP[11]. Therefore, in this research, the influence of different loading methods of Cryo-ECAP on the mechanical properties and conductivity of single crystal copper was investigated.

## 1 Experiment

Single crystal rods of high-purity (99.999%) copper were prepared by Ohno continuous casting method. The rods were cut into the specimens with diameter of 16 mm and length of 65 mm by wire cutting. The specimens were cooled sufficiently in liquid nitrogen, and the die surface and channels were sprayed by liquid nitrogen. Then, the specimens were placed in the ECAP die for ECAP process by route A, route $B_C$, and route C. The microstructures and morphologies of the extruded specimens were observed by optical microscope (OM) and scanning electron microscope (SEM). The texture evolution was detected by X-ray diffractometer (XRD) and electron backscattered diffractometer (EBSD). The hardness of specimens after ECAP was tested by HV-1000 hardness tester. Five points were evenly selected from the central to the outer circumference of each specimen and the average hardness was used for analysis. Tensile tests were conducted by WDW-300 microcomputer-controlled electronic universal testing machine. The conductivity was measured by Sigma 2008B/C digital eddy current metal conductivity meter. Each specimen was measured 5 times and the average conductivity was used for analysis. The schematic diagram of ECAP die and extrusion specimen is shown in Fig.1.

## 2 Results and Discussion

### 2.1 Effect of deformation path on microstructure

Fig. 2 shows EBSD morphologies of single crystal copper after Cryo-ECAP of 4 passes through route A, route $B_C$, and route C. After Cryo-ECAP deformation by route A, a small number of (001) filamentous textures with a large difference in orientation from the basal plane are generated. The strong (001) ribbon texture is formed in the matrix with proportion of about 50% after Cryo-ECAP deformation by route C. However, the misorientation is small, and the microstructure is uniform after Cryo-ECAP deformation by route $B_C$. Shear bands can be clearly observed in all specimens after deformation through different paths due to the pure shear mode of ECAP. However, the formation of shear bands is significantly influenced by the initial crystal orientation, slip surface, and slip direction[18]. A large amount of strain rapidly accumulates, and the strong interactions between (001) texture and basal plane result in the high-density dislocations in the microstructure after Cryo-ECAP of 4 passes through route A. Due to the rotation of 90° in route $B_C$, the microstructure becomes uniform, but the interactions of dislocations become strong after Cryo-ECAP of 4 passes. Because the shear direction of adjacent passes is opposite in route C, the shear bands are offset by each other, resulting in the dispersed orientations. According to the misorientation distributions of grain boundaries in Fig. 3, it can be seen that the low angle grain boundaries (LAGBs, $0° < \theta < 10°$) are dominant in the specimens after Cryo-ECAP of different routes, indicating that the good single crystal microstructure is maintained. The high angle grain boundaries (HAGBs, $\theta \geqslant 10°$) account for a small part in all specimens.

### 2.2 Grain orientation analysis

XRD patterns of single crystal copper processed by Cryo-ECAP are shown in Fig. 4. With increasing the extrusion passes, the primary (111) slip system of initial single crystal copper becomes weak and the intensity of (220) diffraction

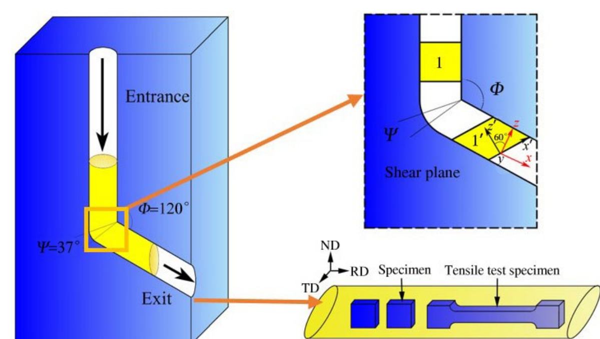


Fig.1 Schematic diagram of ECAP die and extrusion specimen (ND: normal direction; TD: transverse direction; RD: rolling direction)

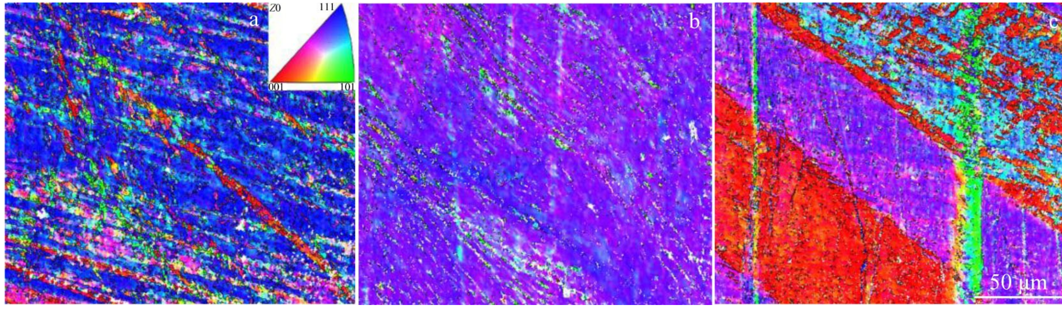


Fig.2 EBSD morphologies of single crystal copper after Cryo-ECAP deformation of 4 passes through route A (a), route $B_C$ (b), and route C (c)

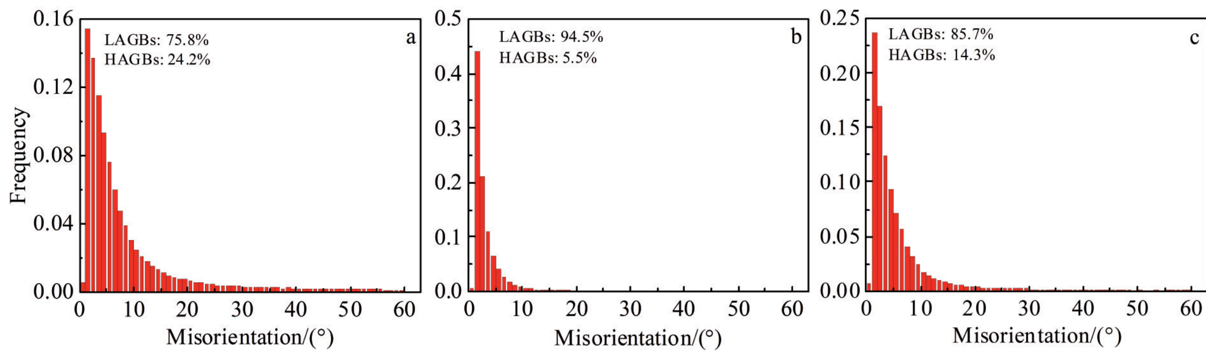


Fig.3 Grain boundary distributions of single crystal copper after Cryo-ECAP deformation of 4 passes through route A (a), route $B_C$ (b), and route C (c)

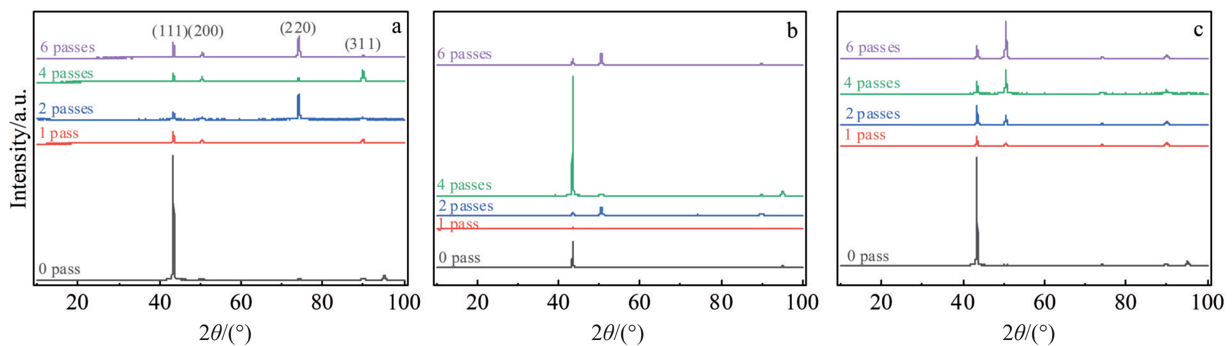


Fig.4 XRD patterns of single crystal copper after Cryo-ECAP through route A (a), route $B_C$ (b), and route C (c)

peak is increased. According to Fig. 4c, the initial (111) orientation does not change significantly. However, the intensity of (200) diffraction becomes stronger with increasing the extrusion passes. This result suggests that the initial orientation of the single crystal copper does not change during the deformation at low-to-intermediate strain (ECAP of 1−4 passes) through route A and route C. The distributions of grain misorientation are basically the same after Cryo-ECAP of route A and route C, as shown in Fig.5a and 5c, respectively. The grain boundary misorientation of single crystal copper deformed through Cryo-ECAP of route $B_C$ is mainly around 1.5° . It is concluded that the accumulation effects of dislocations during the initial several passes of deformation through route A and route C are similar due to the approximately equal strain rates at low strains. Due to the almost uniform orientations of the geometrically necessary grain boundaries during deformation by route A, the dislocation slip is blocked by dislocation plugging, thereby resulting in a large amount of high-density dislocation plugging and large critical initiation stress. Because of the stronger interactive cutting effect of dislocations during the deformation by route C, the accumulation effect of dislocations is partially offset, whereas the accumulative strain is stronger near the central shear plane than that during the deformation by route A. Therefore, the peak misorientation of single crystal copper deformed by route C is larger than that by route A. Additionally, the tensile fractures of single crystal copper deformed through route A are more even than those through route C. In conclusion, after Cryo-ECAP process with intermediate strain, the high-density dislocation plugging appears inside the shear bands of the single crystal copper deformed by route A, the strong interactions between

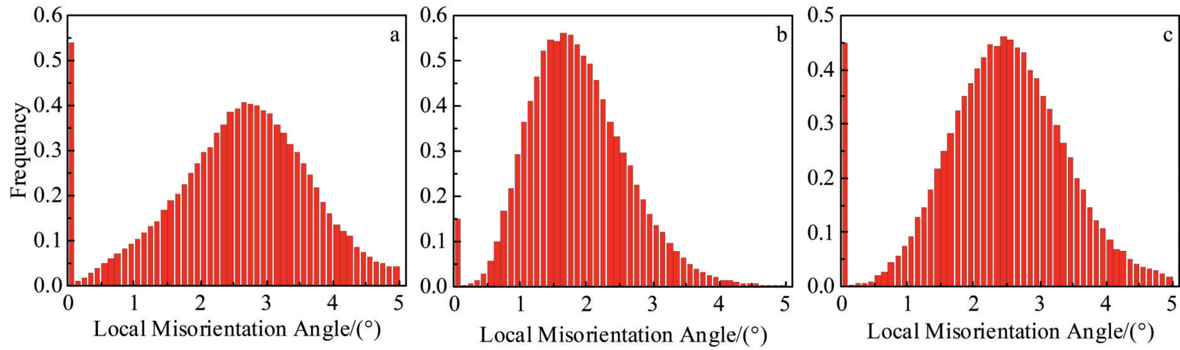


Fig.5 Misorientation distributions of single crystal copper after Cryo-ECAP of 4 passes through route A (a), route $B_C$ (b), and route C (c)

dislocations occur in the single crystal copper deformed by route $B_C$, and the shear bands are gradually dispersed in the single crystal copper deformed by route C. The shear mode of route A is more conducive to the formation of oriented shear bands in the single crystal microstructure and can promote the formation of nano-twins bundles within the single crystal copper.

The dislocation density can be calculated by the Kubin and Morernsen method[19–20], as follows:

$$\rho = 2\theta_{ave}/\mu b \quad (1)$$

$$\theta_{ave} = \exp\left(\frac{1}{N}\sum_{1}^{i}\ln\theta_{1,i}\right) \quad (2)$$

where $\theta_{ave}$ is average misorientation; $b$ is the value of Burgers vector of 0.255[21]; $\mu$ is EBSD scan step of 300 nm; $\theta$ is average misorientation; $N$ is the total number of grains counted. The dislocation density after Cryo-ECAP of 4 passes through route A, route $B_C$, and route C can be calculated as $\rho_A$=1.157×$10^{15}$/m$^2$, $\rho_{B_C}$=8.498×$10^{14}$/m$^2$, and $\rho_C$=1.104×$10^{15}$/m$^2$, respectively. Therefore, they can be arranged as $\rho_A>\rho_C>\rho_{B_C}$. It can be seen that the extruded specimen is not rotated per pass during ECAP by route A, so the accumulative strain of microstructure is increased with increasing the deformation passes, resulting in the high dislocation density. With the rotation of 90° of specimen during each pass by route $B_C$, the strains caused by shear deformation are offset by each other within the material, leading to the lowest accumulated dislocation density.

### 2.3 Texture evolution

Fig. 6 shows the polar figures of single crystal copper deformed by Cryo-ECAP of 4 passes through different routes. The strongest orientation is between the {111} and {100} crystal plane families, and the extreme density is about 16 for the single crystal copper deformed by route A and route C. However, the strongest orientation is {111} with the extreme density of 45.65 for the single crystal copper deformed by route $B_C$, indicating that the deformation through route $B_C$ is still dominated by (111).

Fig. 7 shows the orientation distribution functions of single crystal copper deformed by Cryo-ECAP of 4 passes through different routes. The {111} <110> and {111} <112> textures are formed during Cryo-ECAP through route $B_C$. The {111} <112> and {112} <111> textures are strong during the deformation by route $B_C$. The stronger {110}<112> and

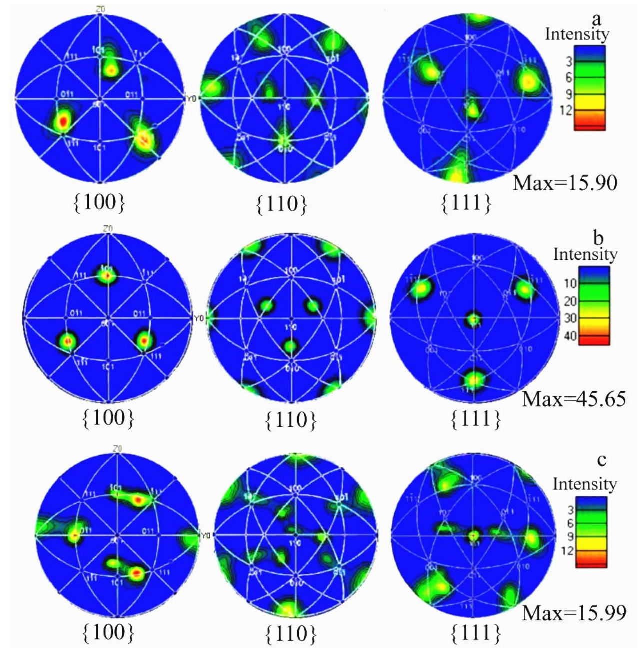


Fig.6 Pole figures of single crystal copper after Cryo-ECAP of 4 passes of through A (a), route $B_C$ (b), and route C (c)

{001}<100> textures appear during Cryo-ECAP through route C, but the {111}<112> and {111}<110> textures are formed at $\phi_2$=45°.

### 2.4 Schmid factor

Fig.8 shows the Schmid factor distributions of single crystal copper deformed by Cryo-ECAP of 4 passes through different routes. Combining with Fig. 2, the Schmid factor of 0.45 accounts for the maximum frequency of 10.08%, which suggests that the deformation is dominated by the primary slip system[22] and the {111} crystal plane is preferentially initiated during Cryo-ECAP by route A. The Schmid factor is mainly concentrated at 0.30, which accounts for 19.06% during Cryo-ECAP by route $B_C$, and the {111} crystal plane is the preferentially initiated slip system. The Schmid factor is concentrated at 0.30 and 0.45 during deformation by route C, which suggests that the preferred slip systems for initiation are {111} and {100} crystal planes during deformation by route C. It can be seen that the single crystal microstructure under intermediate stress is dominated by the {111} basal

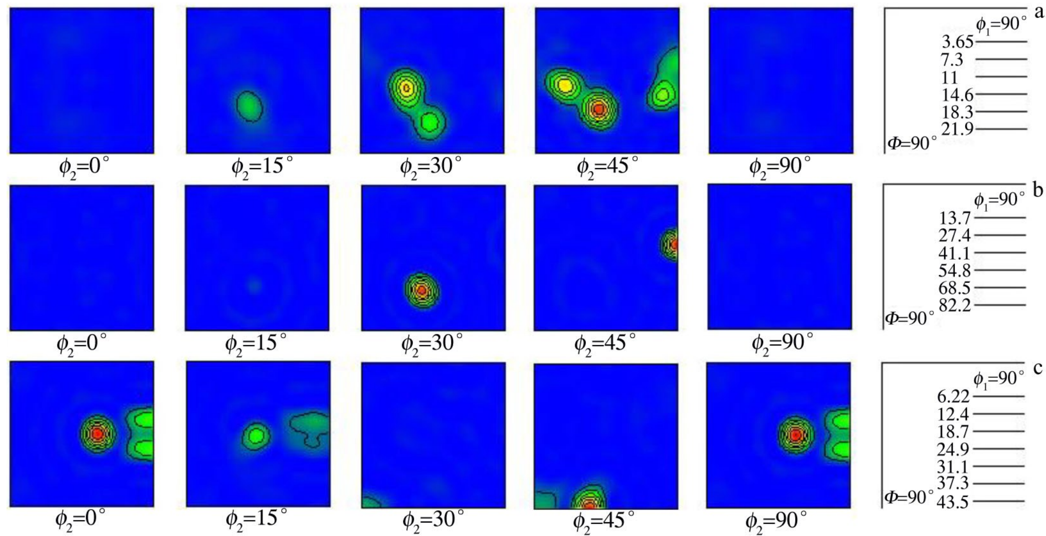


Fig.7 Orientation distribution functions of single crystal copper after Cryo-ECAP of 4 passes through different routes: (a) route A, (b) route $B_C$, and (c) route C

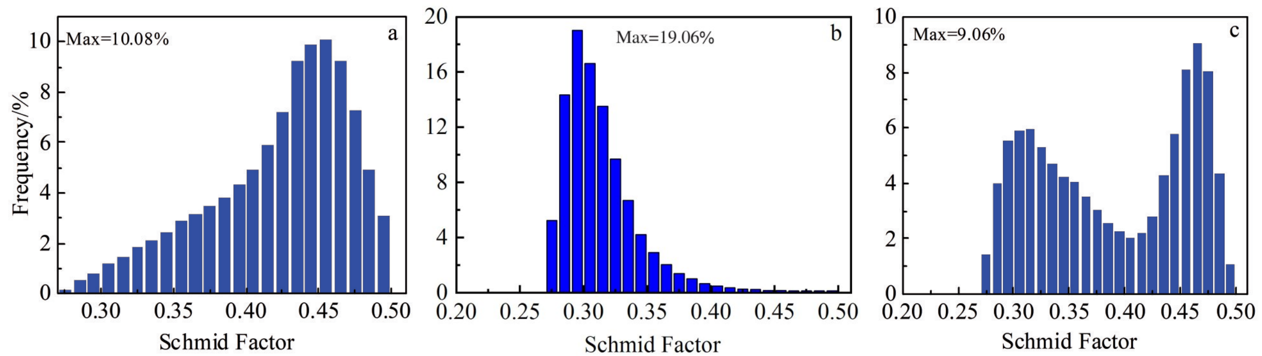


Fig.8 Schmid factor distributions of single crystal copper after Cryo-ECAP of 4 passes by different routes: (a) route A, (b) route $B_C$, and (c) route C

orientation, and the {100} plane slip system exists during the deformation by route C, which is consistent with the evolution result from XRD and texture analyses.

## 2.5 Mechanical properties

Fig. 9 shows the tensile strength, elongation, and hardness of single crystal copper processed by Cryo-ECAP of different passes through different routes. According to Fig.9a, the initial tensile strength of single crystal copper is 126.0 MPa. Then, the tensile strength increases sharply after Cryo-ECAP of 1 pass. The tensile strength of single crystal copper after Cryo-ECAP of 6 passes through route A, route $B_C$, and route C is 400.2, 383.4, and 377.0 MPa, respectively. The initial elongation of single crystal copper is 39.5%. However, the elongation of single crystal copper after Cryo-ECAP of 6 passes through route A, route $B_C$, and route C reaches 13.7%, 12.1%, and 14.6%, respectively. According to Fig. 9b, the

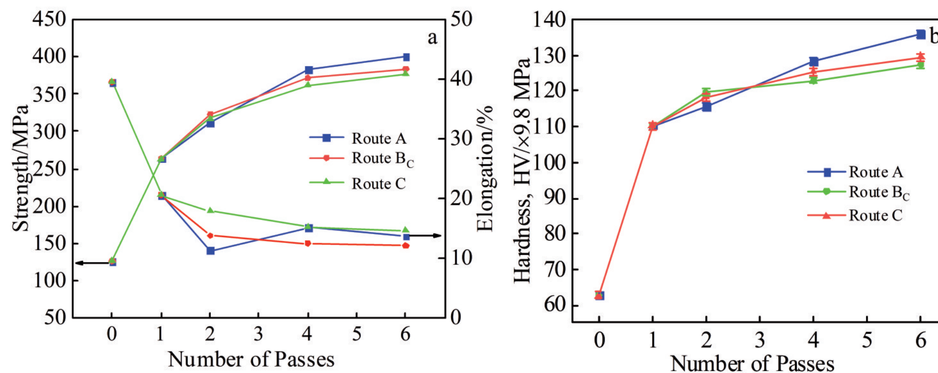


Fig.9 Mechanical properties of single crystal copper deformed by different Cryo-ECAP processes: (a) tensile strength and elongation; (b) hardness

initial hardness of the single crystal copper is 614.5 MPa and it is increased significantly with increasing the number of Cryo-ECAP passes. After Cryo-ECAP of 6 passes through route A, route $B_C$, and route C, the hardness reaches 1333.8, 1249.5, and 1268.1 MPa, respectively.

It can be found that after deformation of 4 passes, the elongation of single crystal copper is above 12% and the tensile strength is above 350 MPa. This is mainly due to the formation of nanofiber microstructure inside the material during deformation, which effectively inhibits the movement of dislocation. After Cryo-ECAP of 4 passes, the accumulated strain inside the material increases and the dislocation can hardly be generated. Thus, higher stresses are required to initiate the new dislocation sources. For the pure single crystal, the yield strength $\tau_c$ can be calculated by Eq.(3–5)[23], as follows:

$$\tau_c = \max(\tau_m, \tau_s) = \max(\tau_f + \tau_{dis}, \tau_s) \tag{3}$$

$$\tau_{dis} = a\mu b\sqrt{\rho_{dis}} \tag{4}$$

$$\tau_s = K\mu b d^{-m} \tag{5}$$

where $\tau_m$ denotes the stress required for dislocation motion; $\tau_s$ is the contribution of dislocation source strengthening; $\tau_f$ is the lattice friction stress; $\tau_{dis}$ is the dislocation source strengthening stress; $a$ is the lattice constant; $\mu$ is the shear modulus; $\rho_{dis}$ is the dislocation density; $d$ is the grain size; $K$ and $m$ are material parameters related to the stacking fault energy, temperature, dislocation source density, etc. Normally, $\tau_m$ depends on $\tau_f$ and $\tau_{dis}$. The values of these parameters are shown in Table 1.

The calculation shows that $\tau_s \ll \tau_m$, which suggests that the yield strength after extrusion of 4 passes mainly depends on the size of internal dislocation density of the material. The dislocations inside the material are entangled with each other after Cryo-ECAP, which seriously inhibits the dislocation slip. The Hall-Petch yield strength of singer crystal copper after extrusion of 4 passes through route A, route $B_C$, and route C is 146.5, 124.2, and 141.5 MPa, respectively, which agrees well with the extrusion characteristics of each route. Due to the difference in dislocation plugging on the shear plane caused by different extrusion routes, the mechanical properties of single crystal copper are quite different after different Cryo-ECAP processes.

Due to the highest density of dislocations caused by directional shear, the material deformed by route A has a high tensile strength. Because there is a rotation interval of 90° between each pass during deformation by route $B_C$, the shear plane is subjected to orthogonal shear stresses during the deformation process and the accumulative strain on the material after the same pass is smaller to that through other routes. During deformation by route C, the specimen is rotated of 180° per pass, resulting in the cross-cutting effects on the shear surface. The interaction (annihilation or recombination) of dislocations caused by alternating stresses between adjacent passes leads to a lower dislocation density, so the mechanical properties of singer crystal copper after deformation by route C is intermediate[25]. With increasing the extrusion passes, the dislocation entanglement and the interaction between dislocations and grain boundaries are enhanced. Therefore, the mechanical properties of the single crystal copper after deformation by route A are superior to those by route $B_C$ and route C, which exerts stronger strain strengthening effect after multi-pass extrusion.

**Table 1 Parameters used for yield stress calculation**

| Parameter | Value | Ref. |
|---|---|---|
| Lattice constant, $a$/nm | 0.3620 | [24] |
| Shear modulus, $\mu$/GPa | 46 | [24] |
| Dislocation density, $\rho_{dis}$/m$^{-2}$ | $1.157\times10^{15}$ (route A)<br>$8.498\times10^{14}$ (route $B_C$)<br>$1.104\times10^{15}$ (route C) | This work |
| Grain size, $d$/$\mu$m | 42 (route A)<br>57 (route $B_C$)<br>64 (route C) | This work |
| $K$/m$^{m-1}$ | 17 | [23] |
| $m$ | 0.9 | [23] |

Fig. 10 shows the fracture morphologies of single crystal copper after Cryo-ECAP of different passes through different routes. Fig. 10a and 10b show that the laminar bumps and numerous dimples appear in the fracture morphologies of single crystal copper after single-pass deformation, and they are not uniformly distributed. This is mainly because many subgrains appear inside the single crystal copper after single-pass extrusion. The specimen fractures along the subgrain boundaries during stretching, resulting in the laminar bumps. As shown in Fig. 10c and 10d, the fracture plane flatness is improved after route A of 6 passes, and the number of dimples is reduced with even distribution. These phenomena indicate that with increasing the extrusion passes, the effect of strain strengthening is increased due to the grain refinement, and the fracture characteristic is transformed from ductile fracture to brittle fracture during the deformation by route A. According to Fig. 10e and 10f, obvious necking phenomenon can be observed after deformation of 6 passes by route $B_C$, indicating the strong plastic fracture characteristic. Tearing characteristics can also be observed. The dimples are reduced, but their depth is increased. As shown in Fig.10g and 10h, less fracture section and larger dimple depth can be observed. Due to different deformation characteristics of each path, there is a small grain misorientation during Cryo-ECAP of 6 passes by route A, whereas the dislocation entanglement during Cryo-ECAP of 6 passes by route $B_C$ and route C is stronger. Thus, the fracture morphologies of single crystal copper deformed through route $B_C$ and route C show more obvious plastic fracture characteristics.

### 2.6 Conductivity

Fig.11 shows the conductivity of single crystal copper after Cryo-ECAP of different passes through different routes. It can be seen that the initial conductivity of single crystal copper is 100.5%IACS. The conductivity decreases to 99.9%IACS after single-pass deformation. With increasing the extrusion passes, the conductivity remains at above 98%IACS. After deformation of 6 passes, the conductivity of single crystal

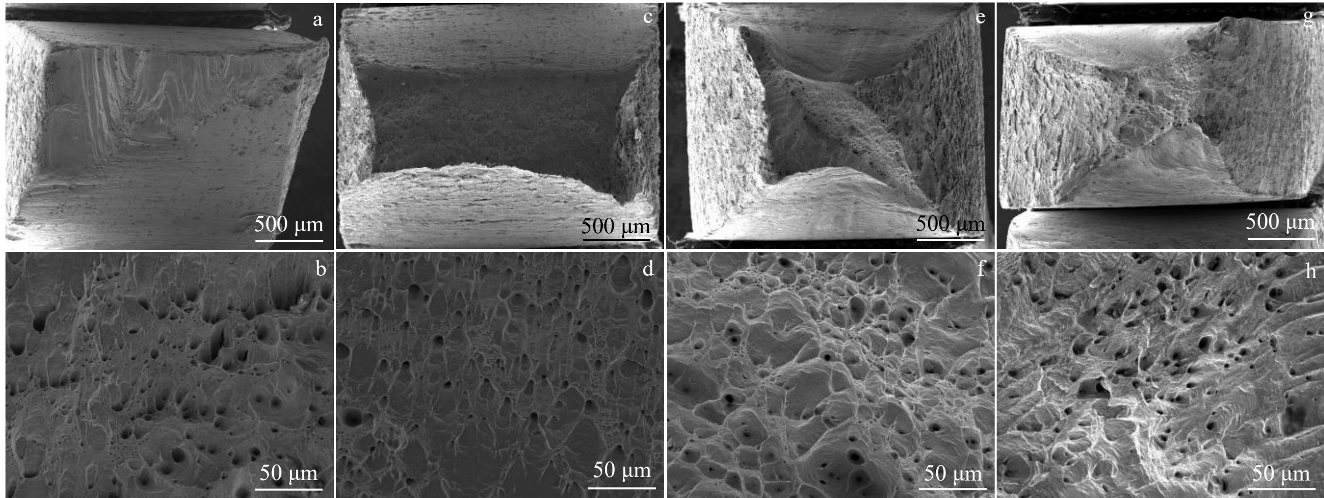


Fig.10 Fracture morphologies of single crystal copper deformed by Cryo-ECAP of 1 pass (a–b) and 6 passes through route A (c–d), route $B_C$ (e–f), and route C (g–h)

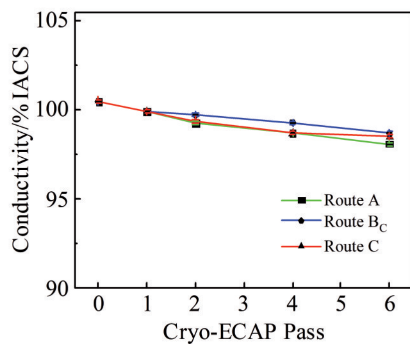


Fig.11 Conductivity of single crystal copper deformed by different Cryo-ECAP processes

copper deformed by route A, route $B_C$, and route C is 98.1%IACS, 98.7%IACS, and 98.5%IACS, respectively. Therefore, the influence degree of ECAP deformation on conductivity can be arranged as route $B_C$>route C>route A. Ref. [26 – 27] reported that the conductivity of directionally solidified single crystal copper is 98.3%IACS and 94.5%IACS after multi-pass ECAP at room temperature and at cryogenic temperature, respectively, indicating that Cryo-ECAP can significantly increase the strength of single crystal copper with slight weakening effect on conductivity.

Due to the elimination of transverse grain boundaries, the single crystal copper is less susceptible to the scattering of electrons, resulting in the high conductivity. With increasing the dislocation density and the number of LAGBs during ECAP, the inferior homogeneity of microstructure slightly promotes the scattering of electrons. With increasing the strain, the conductivity of materials is slightly decreased. The continuous directional-plugging of dislocations on shear plane significantly affects the conductivity during deformation by route A. The orientation of dislocations alternately changes after each pass of route C, resulting in the decreased conductivity. The shear bands alternately change after rotation of 90° during the deformation by route $B_C$, so the conductivity of single crystal copper deformed by route $B_C$ is higher than that deformed by route A and route C. In addition, the {111}<110> texture has less influence on the conductivity of single crystal copper during ECAP at room temperature. Based on the analysis of Schmid factor, it is clear that the {111} slip system is dominant in the multi-pass extrusion, which has less influence on the scattering of electrons. The strong {111} <112> texture maintains the high conductivity during Cryo-ECAP deformation. This influence mechanism is different from that of ECAP at room temperature.

## 3 Conclusions

1) After the cryogenic equal channel angular pressing (Cryo-ECAP) process with intermediate strain, the high-density dislocation plugging appears inside the shear bands of the single crystal copper deformed by route A, the strong interactions between dislocations occur in the single crystal copper deformed by route $B_C$, and the shear bands are gradually dispersed in the single crystal copper deformed by route C. The shear mode of route A is more conducive to the formation of oriented shear bands in the single crystal microstructure and can promote the formation of nano-twins bundles within the single crystal copper.

2) During Cryo-ECAP deformation through different routes, the sliding mode of single crystal copper is dominated by {111}<110> orientation and the strong {111}<112> texture is formed after Cryo-ECAP of 4 passes. The deformed microstructure maintains the excellent single-crystal state, which can effectively improve the strength and slightly decrease the conductivity.

3) The comprehensive mechanical properties of single crystal copper can be significantly improved by Cryo-ECAP deformation. After Cryo-ECAP of 6 passes through route A, route $B_C$, and route C, the tensile strength reaches 400.2, 383.4, and 377.0 MPa, respectively. The maximum yield

strength is 146.5 MPa, the elongation is all above 12%, and the hardness is higher than 1245 MPa after Cryo-ECAP deformation through different routes, indicating that the comprehensive properties are enhanced, compared with those after multi-pass ECAP deformation at room temperature.

4) Single crystal copper processed by Cryo-ECAP has directional shear bands and the high-density dislocations are generated. The dislocation entanglement effectively inhibits the dislocation slip, while the grains maintain the excellent characteristics of single crystal material, therefore maintaining the high conductivity and high strength of single crystal copper.

## References


1 Guo T B, Wang C, Li Q *et al. Rare Metal Materials and Engineering*[J], 2019, 48(4): 1065
2 Wang H, Lu C, Tieu K. *Journal of Materials Research and Technology*[J], 2019, 8(6): 5057
3 Gao L, Chen R S, Han E H. *Journal of Alloys and Compounds*[J], 2009, 481(1–2): 379
4 Lu K, Lu L, Suresh S. *Science*[J], 2009, 324(5925): 349
5 Pry R H, Hennig R W. *Acta Metallurgica*[J], 1954, 2(2): 318
6 Xiao Z, Wang W Y, Lei Q *et al. Journal of Alloys and Compounds*[J], 2021, 894: 162 284
7 Zhu Y T, Liao X Z. *Nature Materials*[J], 2004, 3(6): 351
8 Meyers M A, Mishra A, Benson D J. *Progress in Materials Science*[J], 2006, 51(4): 427
9 Jayakumara P K, Balasubramaniana K, Rabindranath T G. *Materials Science and Engineering A*[J], 2012, 538(3): 7
10 Tao Nairong, Lu Ke. *Acta Metallurgica Sinica*[J], 2014, 50(2): 141 (in Chinese)
11 Wu Shiding, An Xianghai, Han Weizhong *et al. Acta Metallurgica Sinica*[J], 2010, 46(3): 257 (in Chinese)
12 Higuera-Cobos O F, Cabrera J M. *Materials Science and Engineering A*[J], 2013, 571: 103
13 Fukuda Y, Oh-Ishi K, Furukawa M *et al. Journal of Materials Science*[J], 2007, 42(5): 1501
14 Shin D H, Pak J J, Kim Y K *et al. Materials Science and Engineering A*[J], 2002, 323(1–2): 31
15 Li M Q, Zhang C, Luo J *et al. Rare Metals*[J], 2010, 29(6): 613
16 Qin Jia, Yang Xuyue, Ye Youxiong. *Rare Metal Materials and Engineering*[J], 2016, 45(5): 1340 (in Chinese)
17 Chen Y B, Li Y L, He L Z *et al. Materials Letters*[J], 2008, 62(17–18): 2821
18 Katayama S, Miyamoto H, Vinogradov A *et al. Materials Science Forum*[J], 2008, 584–586: 387
19 Hansen N. *Scripta Materialia*[J], 2004, 51(8): 801
20 Wang Y B, Liao X Z, Zhao Y H *et al. Materials Science and Engineering A*[J], 2010, 527(18–19): 4959
21 Derakhshan J F, Parsa M H, Ayati V *et al. American Institute of Physics Conference Proceedings*[C]. Lausanne: AIP Publishing LLC, 2018, 1920(1): 20 025
22 Liu W B, Liu Y, Cheng Y Y *et al. Physical Review Letters*[J], 2020, 124(23): 235 501
23 Liu Y, Li Z, Jiang Y X *et al. Journal of Materials Research*[J], 2017, 32(7): 1324
24 Peng L J, Xie H F, Huang G J *et al. Journal of Alloys and Compounds*[J], 2017, 708: 1096
25 Furukawa M, Horita Z, Langdon T G. *Materials Science and Engineering A*[J], 2002, 332(1–2): 97
26 Guo T B, Wei S R, Li Q *et al. Materials and Technology*[J], 2019, 53(2): 269
27 Xu J, Li J W, Shan D B *et al. Materials Science and Engineering A*[J], 2016, 664: 114


# 超低温等通道转角挤压高导电单晶铜的霍尔佩奇强化


郭廷彪[1,2]，冯　瑞[1]，李凯哲[1]，高　洋[1]，钱丹晨[1]，贾　智[1,2]，丁雨田[1,2]，凌得魁[3,4]

(1. 兰州理工大学 省部共建有色金属先进加工与再利用国家重点实验室，甘肃 兰州 730050)

(2. 兰州理工大学 材料科学与工程学院，甘肃 兰州 730050)

(3. 金川集团股份有限公司，甘肃 金昌 737100)

(4. 镍钴共伴生资源开发与综合利用全国重点实验室，甘肃 金昌 737100)



**摘　要：**分别采用光学显微镜、扫描电镜、X射线衍射仪和电子背散射衍射分析超低温等通道转角挤压（ECAP）中等应变量单晶铜的形变组织和织构演变，测试材料的力学和导电性能，分析材料组织转变机理及其对材料力学和导电性能的影响。结果表明，超低温ECAP早期形成的定向剪切带在后续变形过程中会严重影响材料组织的转变过程。增加应变量，A路径变形中剪切带内部会形成高密度的位错塞积，特征晶界占比增加；$B_C$路径变形时剪切带内部的位错发生强烈的交互作用；C路径变形后剪切带的取向发生分散。经过6道次变形后，单晶铜组织中形成强烈的{111}<112>织构，材料强度从初始126.0 MPa增加到400.2 MPa，而导电率仍保持在98%IACS以上。低温ECAP变形后组织内部形成定向剪切带并产生高密度的位错，位错间相互缠结，有效阻碍了位错滑移，而晶粒仍保持良好的单晶特性。



**关键词：**单晶铜；超低温等通道转角挤压；微观组织；织构；力学性能；导电率


---


作者简介：郭廷彪，男，1974年生，博士，教授，兰州理工大学省部共建有色金属先进加工与再利用国家重点实验室，甘肃兰州 730050，E-mail：lutguotb@163.com